

## ON THE DETERMINATION OF THE SOLVUS TEMPERATURE IN ALUMINUM ALLOYS USING DIFFERENTIAL SCANNING CALORIMETRY

A.K. Gupta<sup>1</sup>, A.K. Jena<sup>2</sup> and D.J. Lloyd<sup>1</sup>

1. Alcan International Limited, Kingston Research and Development Centre  
Box 8400, 945 Princess Street, Kingston, Ontario, K7L 5L9
2. Indian Institute of Technology, Department of Materials and Metallurgical Engineering  
Kanpur, India, 208016.

### Introduction

Information pertaining to the solvus temperature in heat treatable alloys is required for many purposes, such as alloy selection and design of appropriate heat treatments [1]. Usually, the solvus temperature is determined by using many alloy compositions, each of which is equilibrated at many temperatures and analyzed to determine the composition of co-existing phases. This is a complex and time-consuming method. In this paper, it is shown how one can obtain the solvus temperature using a differential scanning calorimeter. In the calorimeter, a specimen is heated at a constant rate and the heat effects due to precipitation and dissolution reactions occurring in the specimen are recorded [2]. The finish temperature of the precipitation heat effect and the initiation temperature of the dissolution heat effect are normally different. However, if Differential Scanning Calorimetry (DSC) experiments are carefully performed at small heating rates, it is possible to obtain reasonable estimates of the solvus temperatures and compositions. In this paper the determination of solvus temperatures and compositions associated with the S ( $\text{CuMgAl}_2$ ) phase in a ternary Al-1.53%Cu-0.79%Mg alloy and those associated with two different binary Al-Si alloys are discussed.

### Differential Scanning Calorimetry (DSC)

The differential scanning calorimeter normally uses two pans, placed on two raised platforms in the centre of a chamber, which can be heated at a desired rate. One of the pans is the reference pan while the other is the sample pan. The DSC output of a sample-reference run represents the variation in the net heat flow to the reference relative to that to the sample as a function of temperature. The peaks and depressions in the curve represent the precipitation and dissolution reactions respectively.

The DSC experiments were performed according to procedures developed previously [3,4]. Specimens were punched from cold rolled material and solution heat treated by heating to a sufficiently high temperature and quenching into water. The solution heat treated samples were then heated in a DSC cell at heating rates of 5, 10, 15 and 20°C/min, in an argon atmosphere. Each run was performed with pure aluminum as the reference. The weights of the specimens and the reference aluminum were adjusted in a such a manner that their heat capacities were nearly the same. The data obtained from the sample-pure aluminum reference run were subtracted from a pure Al-Al run performed under identical conditions. Each experiment was performed in duplicate, and the results were found to be highly reproducible.

Figure 1 shows the DSC thermograms of a solution heat treated Al-1.53%Cu-0.79%Mg alloy obtained with four heating rates of 5, 10, 15 and 20°C/min. All the curves show two exothermic precipitation and two endothermic dissolution peaks respectively.

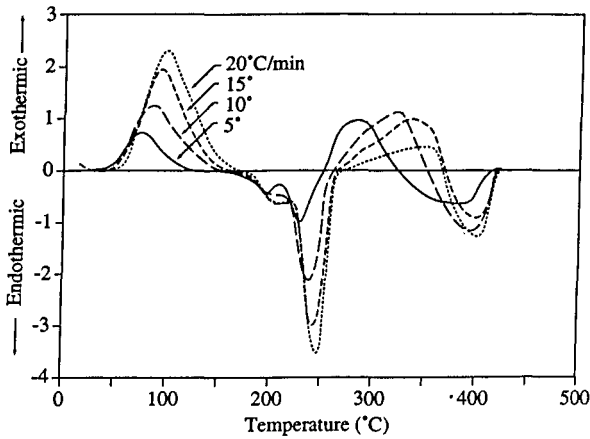


**Figure 1:** DSC curves at heating rates of 5, 10, 15 and 20°C/min for solution treated and quenched specimens of the Al-1.53%Cu-0.79%Mg alloy.

### Results and Discussion

#### Al-1.53%Cu-0.79%Mg Alloy

The first exothermic peak in the thermograms, Figure 1, is due to the formation of GPB zones. The dissolution of GPB zones and complexes form the first endothermic peak. The second exothermic peak is attributed to the precipitation of the S phase, and the following endothermic peak is a result of its dissolution [2].

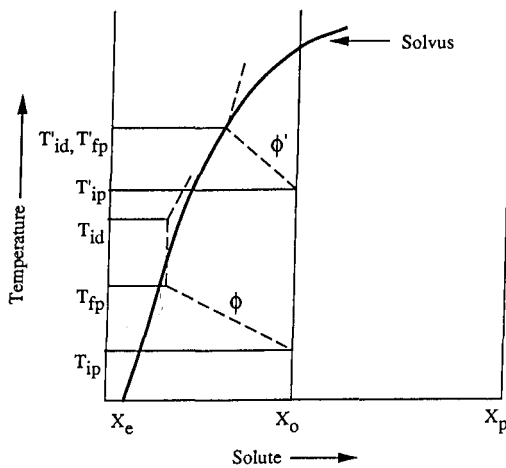


**Figure 2:** Schematic diagram showing the influence of temperature on  $T_{fp}$  and  $T_{id}$

Figure 2 schematically illustrates the variation of the average composition of the matrix during precipitation. The figure shows the solvus composition  $X_e$ , the composition of the super saturated solid solution  $X_0$  and the composition of the precipitate  $X_p$ . When the super saturated solid solution is heated at the constant rate,  $\phi$ , the precipitation reaction may start at  $T_{ip}$  but stop at a temperature  $T_{fp}$ , which is below the solvus temperature because of the small driving force near the solvus temperature. The dissolution process would start at a temperature  $T_{id}$  just above the solvus temperature. Thus, no reaction should be observed in the temperature interval  $T_{fp}$  to  $T_{id}$ . The GPB zone peak in Figure 1 shows such a behaviour. However, if the precipitation reaction occurs at a higher temperature, the reaction at the constant heating rate  $\phi$  may start at  $T'_{ip}$ , finish at the solvus temperature and show the beginning of the dissolution process just above this temperature. In such a situation (Figure 2) there would be negligible difference between  $T'_{ip}$  and  $T_{id}$ , suggesting  $T'_{ip}$  to be the solvus temperature,  $T_e$ . Such a behaviour is observed in the precipitation and dissolution of the S phase. Consequently,  $T_{fp}$  is equal to the solvus temperature  $T_e$  and the corresponding composition,  $X_e$ , is the matrix composition which may be calculated from the amount of precipitation of the S phase that has taken place.

The extent of precipitation of the S phase can be calculated from the total heat effect,  $Q(T_f)$ , accompanying precipitation process. The total heat effect is given by [2]:

$$Q(T_f) = \frac{EA(T_f)}{M\phi} \quad (1)$$

Where

- $Q(T_f)$  = the total heat effect due to precipitation up to peak end temperature  $T_f$  per gram, (J/g)
- $M$  = mass of specimen, (g)
- $\phi$  = heating rate, °C/sec
- $A(T_f)$  = area under the precipitation peak from  $T_i$  to  $T_f$
- $E$  = DSC cell calibration constant

If  $Q_0$  is the heat effect due to precipitation of a g-atom of S precipitate, the number of g-atoms of Cu and those of Mg removed from the matrix by precipitation of the S phase ( $Al_{0.5}Cu_{0.25}Mg_{0.25}$ ) are  $[0.25Q(T_f)M/Q_0]$  each. Hence,  $X$ , the matrix composition at  $T_f$  of the precipitation peak is:

$$X_{Cu} = \left[ \frac{(M \cdot X_{0,Cu} / W) - \{0.25Q(T_f) \cdot M / Q_0\}}{(M / W) - Q(T_f) \cdot M / Q_0} \right] \quad (2)$$

$$\cong X_{0,Cu} - 0.25Q(T_f)W / Q_0$$

where

- $X_{Cu}$  = atom fraction of Cu in the matrix at  $T_f$  of precipitation peak
- $X_{0,Cu}$  = atom fraction of Cu in supersaturated solid solution
- $W$  =  $[\sum f_i W_i]^{-1}$ ,  $i$  is component of the alloy,  $f_i$  is the weight fraction of component  $i$  in the supersaturated solid solution and  $W_i$  is the atomic weight of component  $i$ .

The expression for the Mg content of the matrix at  $T_f$  is similar.

As  $T_f$  is equal to  $T_e$ , the matrix composition at  $T_f$  is equal to the solvus composition  $X_e$ . Hence:

$$T_e = T_f \quad (3)$$

$$X_{e,Cu} = X_{0,Cu} - C \cdot Q(T_f) \quad (4)$$

$$X_{e,Mg} = X_{0,Mg} - C \cdot Q(T_f) \quad (5)$$

where

$$C = (0.25W / Q_0) \quad (6)$$

For obtaining relation between the solvus composition and solvus temperature, we note that the partial free energy of a component in the precipitate is same as that in the matrix in equilibrium with the precipitate. Considering the component Cu,

$$(\bar{H}_{Cu}^m - \bar{H}_{Cu}^p) = T(\bar{S}_{Cu}^m - \bar{S}_{Cu}^p)$$

or

$$(\bar{H}_{Cu}^m - \bar{H}_{Cu}^p) = T(\Delta\bar{S}_{Cu}^{m,ex} - R \ln X_{e,Cu} - \Delta\bar{S}_{Cu}^p) \quad (7)$$

where  $H$  and  $S$  are partial enthalpies and entropies respectively, superscripts  $m$ ,  $p$  and  $ex$  denote matrix in equilibrium with the precipitate, precipitate and excess property respectively and  $R$  is the gas constant. Considering 0.25 g-atom of Cu, Equation (7) reduces to:

$$RT \ln \bar{X}_{e,Cu}^{1/4} = -0.25(\bar{H}_{Cu}^m - \bar{H}_{Cu}^p) + 0.25T(\Delta\bar{S}_{Cu}^{m,ex} - \Delta\bar{S}_{Cu}^p) \quad (8)$$

combining Equation (8) with similar equations derived for 0.25 g-atom of Mg and 0.5 g-atom of aluminum, we obtain,

$$\ln X_{e,Al}^{1/2} X_{e,Mg}^{1/4} X_{e,Cu}^{1/4} = -\frac{\Delta H}{RT} + \Theta \quad (9)$$

where

$$\Delta H = 0.5(\bar{H}^m - \bar{H}^p)_{Al} + 0.25(\bar{H}^m - \bar{H}^p)_{Cu} + 0.25(\bar{H}^m - \bar{H}^p)_{Mg}$$

and

$$\Theta = \frac{1}{R} \left[ 0.5(\Delta\bar{S}^{m,ex} - \Delta\bar{S}^p)_{Al} + 0.25(\Delta\bar{S}^{m,ex} - \Delta\bar{S}^p)_{Cu} + 0.25(\Delta\bar{S}^{m,ex} - \Delta\bar{S}^p)_{Mg} \right]$$

It should be noted that  $\Delta H$  is the heat effect due dissolution of a g-atom of  $S$  phase in the matrix of solvus composition.

The Al-1.53wt%Cu-0.79wt%Mg alloy contains 0.655at%Cu and 0.883at%Mg. Hence,  $X_{Al} = 0.985$  and  $X_{Al}^{1/2} = 0.993 \sim 1$ . Equation (9) may now be written as:

$$\ln X_{e,Cu} X_{e,Mg} = -\frac{4\Delta H}{RT} + 4\Theta \quad (10)$$

Substituting from Equations (4) and (5),

$$\ln \left[ X_{0,Cu} - C \cdot Q(T_f) \right] \left[ X_{0,Mg} - C \cdot Q(T_f) \right] = -\frac{4\Delta H}{RT_f} + 4\Theta \quad (11)$$

The values of  $Q(T_f)$  and  $T_f$  were experimentally determined by DSC as a function of heating rate. The values are listed in Table 1.

Table I. The total heat effects and peak finishing temperatures values determined experimentally from DSC run obtained at different heating rates.

Heating Rate °C/min	Q(T <sub>p</sub> ), J/g	T <sub>fp</sub> , °C
5	8.3	320
10	5.5	348
15	3.4	364
20	1.3	368

The results are plotted in Figure 3 after Equation (11) with a value of 0.001 for the constant C, such that the plot is linear with a minimum scatter. Also the selected value of C yields a reasonable value of 6800 J/g-atom for Q<sub>0</sub>.

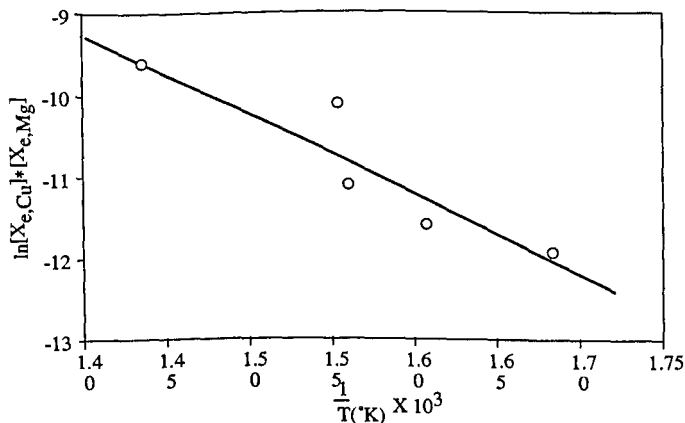


Figure 3: The solvus line of the S phase in an Al-1.53%Cu-0.79%Mg alloy

Figure 1 further shows that the thermogram at four different heating rates show the same T<sub>f</sub> value for the last dissolution peak. It implies that T<sub>f</sub> = T<sub>e</sub> and X<sub>e</sub> = X<sub>0</sub>. The DSC yields the following values for those parameters:

$$X_{Cu} = X_{0,Cu} = 0.00655$$

$$X_{Mg} = X_{0,Mg} = 0.00883$$

$$T_e = 427 \pm 3^\circ\text{C/min}$$

This point is also plotted in Figure 3.

The solute contents of the matrix in equilibrium with the S phase have been determined by Little et al [5]. These results are shown as the line in Figure 3. The results obtained from DSC and those determined by Little et al are in very good agreement with each other. The value of  $\Delta H$  obtained from the slope is -19,600 J/g-atom which is also reasonable.

#### Al - Si Alloy

Figure 4 shows thermograms (a) and (b) obtained by heating solution heat treated Al-0.4%Si and Al-0.9%Si alloys at 10°C/min respectively. Each of these DSC curves show an exothermic and an endothermic peaks representing precipitation and dissolution of Si respectively. In these alloys also T<sub>fp</sub> and T<sub>id</sub> are the same. Therefore, T<sub>e</sub> = T<sub>f</sub> corresponding to the matrix composition that can be obtained from the measured heat effects after Equation (1).

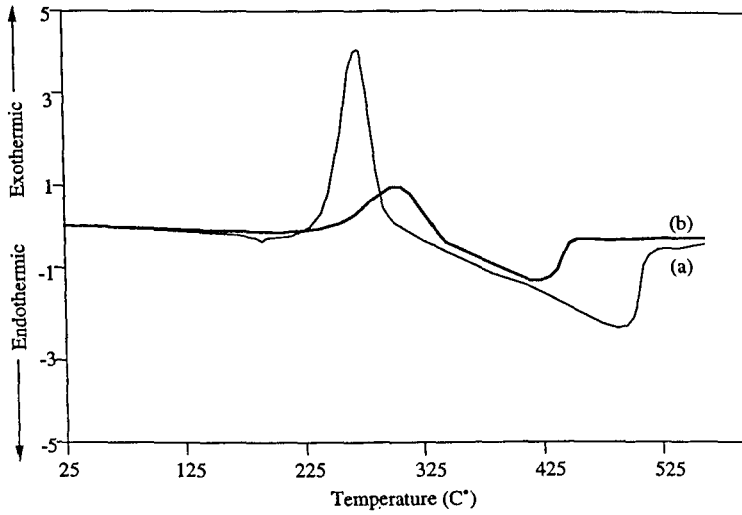


Figure 4: DSC curves of Al-Si alloys solution heat treated at 560°C/min for 5 minutes and quenched in to water (a) Al-0.9%Si (b) Al-0.4%Si

Using the procedure described earlier,

$$T_e = T_f \quad (12)$$

$$X_{e,si} = X_{0,si} - C \cdot Q(T_f) \quad (13)$$

where

$$C = (W / Q_0) \quad (14)$$

when pure Si is in equilibrium with the Al-Si solid solution,

$$\bar{H}_{Si} - T\bar{S}_{Si} = \bar{H}_{Si}^0 - T\bar{S}_{Si}^0 \quad (15)$$

proceeding as before:

$$\ln X_{e,si} = -\frac{\Delta H}{RT} + \Theta \quad (16)$$

where

$$\Delta H = \Delta \bar{H}_{Si}$$

$$\Theta = \left( \frac{\Delta \bar{S}^{ex}}{R} \right)$$

Substituting from Equations (12) and (13)

$$\ln [X_{0,si} - C \cdot Q(T_f)] = -\frac{\Delta H}{RT_f} + \Theta \quad (17)$$

DSC data for  $Q(T_f)$  and  $T_f$  obtained with Al-0.4%Si and Al-0.9%Si alloys are listed below in Table 2.

Table II. The total heat effects and peak finishing temperatures values determined experimentally from DSC run obtained at different heating rates.

Heating Rate, °C/min	0.4%Si		0.9%Si	
	Q(T <sub>f</sub> ), J/g	T <sub>f</sub> , °C	Q(T <sub>f</sub> ), J/g	T <sub>f</sub> , °C
5	4.3	323	11.0	329
10	4.2	338	11.4	332
15	4.1	348	10.8	333
20	3.6	357	11.0	343

These results are plotted in Figure 5 according to Equation (17) with values of C such that the plots are linear for 0.4 and 0.9%Si alloys. The two C values for the two alloys yield a reasonable value of 38514 J/g-atom for Q<sub>0</sub>.

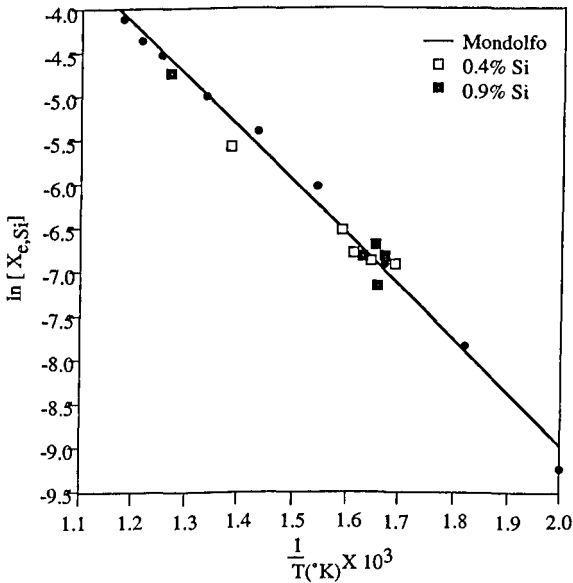


Figure 5: The solvus line of the Si particles in an Al-Si alloy

The thermograms of the two alloys further show that  $T_{fd}$  is independent of heating rate. Hence,  $T_f = T_e$  corresponding to the solvus composition  $X_e$  which is equal to the supersaturated alloy composition. Hence:

For the Al-0.4%Si alloy;

$$T_e = 452^\circ\text{C}$$

$$X_{Si} = X_{0, Si} = 0.0038$$

For the Al-0.9%Si alloy:

$$T_e = 517^\circ\text{C}$$

$$X_{Si} = X_{0, Si} = 0.0086$$

These points are also plotted in Figure 5.

The Si content of the Al-Si alloy solid solution in equilibrium with the Si are available in the literature [6]. These results are shown as a straight line in Figure 5. The DSC results are thus in agreement with those reported in the literature [6]. The slope of the straight line gives a reasonable value of  $-46000$  J/g-atom for  $\Delta\bar{H}_{si}$ .

#### Summary and Conclusions

DSC experiments were performed on solution heat treated Al-1.53%Cu-0.79%Mg, Al-0.4%Si and Al-0.9%Si alloys. Heat effects of precipitation peaks and the final peak temperatures,  $T_f$  of the precipitation and dissolution peaks were measured. Matrix compositions were calculated from the heat effects. Relations between solvus compositions and solvus temperatures were developed. The DSC results yielded solvus temperatures and compositions which are in good agreement with the solubility data available in the literature.

#### References

1. G. Lorimer, in 'Precipitation Processes in Solids', Edited by K.C. Russell and H.I. Aaronson, TMS, AIME (1978), 88.
2. A.K. Jena, A.K. Gupta, and M.C. Chaturvedi, M.C., Acta Met., (1989), 37, 385.
3. A.K. Gupta, Ph.D. Thesis, The University of Manitoba, Canada, (1987).
4. A.K. Gupta, A.K. Jena, and D.J. Lloyd, Presented at QCMR Retreat, Toronto, (1992).
5. A.T. Little, W. Hume-Rothery, and G.V. Raynor, J. Inst. Met., (1951), 79, 321.
6. L.F. Mondolfo, Aluminum Alloys: Structure and Properties, Butterworths (1976), 369.